

Measurements of the radial profile of magnetic field in the Gas-Dynamic Trap using a motional Stark effect diagnostic

P. A. Bagryansky, P. P. Deichuli, A. A. Ivanov, S. A. Korepanov, A. A. Lizunov,
S. V. Murakhtin, and V. Ya. Savkin

Budker Institute of Nuclear Physics, 11 Academician Lavrentiev prospect, Novosibirsk 630090, Russia

D. J. Den Hartog^{a)} and G. Fiksel

Department of Physics, University of Wisconsin-Madison, Madison, Wisconsin 53706

(Presented on 8 July 2002)

We have implemented a spectral motional Stark effect diagnostic for spatially localized measurements of magnetic field on the Gas-Dynamic Trap (GDT) magnetic mirror device. A 7 A, 40 keV diagnostic neutral hydrogen beam was focused to a current density of 0.25 A/cm² in the measurement volume, allowing achievement of a radial resolution of 4.5 cm by viewing the beam at 45° with a well-defined light collection chord. The entire Stark spectrum was recorded by a spectrometer with a charge-coupled device detector. Analysis of the splitting of the components of the Stark spectrum directly results in a measurement of local $|\mathbf{B}|$. When operated with deuterium heating neutral beam injection into a hydrogen target plasma, the GDT axial magnetic field is strongly perturbed by plasma diamagnetic effects. Thus, measurement of the radial profile of the perturbed magnetic field, combined with equilibrium modeling, will yield an estimate of the plasma beta. © 2003 American Institute of Physics. [DOI: 10.1063/1.1527260]

I. INTRODUCTION

The Gas-Dynamic Trap (GDT) is a long axially symmetric mirror system with a high mirror ratio (Fig. 1) for confinement of a two-component plasma.¹ The first component is a collisional target plasma with ion and electron temperatures up to 120 eV and density up to $1.8 \times 10^{20} \text{ m}^{-3}$. The mean free path for scattering target plasma ions into the loss cone is much less than mirror-to-mirror distance, thus target ion confinement can be modeled as an ideal gas confined in a box with a pinhole leak. The second component is a fast ion minority with a mean energy of 5–10 keV and density up to 10^{19} m^{-3} , produced by 45° neutral beam injection. The fast ions are confined in the collisionless mirror regime, and their turning point corresponds to a mirror ratio of 2.

The critical issue for feasibility of a neutron source based on a gas-dynamic trap is stable confinement of a high density of fast ions with a small angular distribution.² The axial and radial profiles of plasma pressure (or plasma β) near the fast ion turning points determines the spatial profile of neutron flux in the testing zones of a projected GDT-based neutron source.² Profiles of plasma β can be constructed by measuring the profile of the diamagnetic perturbation of the confining axial magnetic field in GDT, and combining these measurements with equilibrium modeling. The first single-point motional Stark effect (MSE) measurement of the perturbed magnetic field in GDT was reported in Ref. 3. Here, we report improvement in accuracy and extension of the technique to measurement of a radial profile of the perturbed magnetic field.

II. SPECTRAL MOTIONAL STARK EFFECT DIAGNOSTIC ON THE GAS-DYNAMIC TRAP

The Stark effect is a result of the breaking of energy-level degeneracy of an atom in an external electric field. In the frame of reference of an atom moving transverse to a magnetic field, a Lorenz electric field $\mathbf{E} = (\mathbf{v} \times \mathbf{B})$ appears, causing the energy levels to split. For a hydrogen (or hydrogen-like) atom the resulting Stark splitting is linear in electric field, thus providing a robust method of magnetic-field measurement. The H_α line (656.28 nm) emitted by the diagnostic neutral beam atoms was chosen for MSE measurements on the GDT experiment. For typical GDT magnetic-field values of 0.4–0.5 T and beam velocity of $2.7 \times 10^6 \text{ m/s}$, other effects (Zeeman splitting, fine structure of atom energy levels, and other relativistic corrections) contribute negligibly to line splitting compared to Stark splitting. Thus, a model including only the Stark effect was used for analysis of the recorded MSE spectrum.⁴ The local magnetic field was determined by fitting a model Stark profile to a measured beam emission spectrum, a technique similar to that employed for spectral MSE diagnostics on Madison Symmetric Torus (MST)⁵ and Torus Experiment for Technology Oriented Research (TEXTOR).⁶

The MSE diagnostic setup on GDT is shown in Fig. 2. The diagnostic is comprised of the neutral beam injector Diagnostic Injector of Neutral Atoms-5M (DINA-5M)⁷ and an optical system for collection, dispersion, and recording of the beam emission. Figure 3 shows a schematic of the DINA-5M injector. The main parameters of the diagnostic injector are presented in Table I. A small beam diameter at the focal plane and a high beam current fraction at the full injection energy of 40 keV make the DINA-5M injector the appropriate instrument for application to space-resolved MSE mea-

^{a)}Electronic mail: djdenhar@wisc.edu

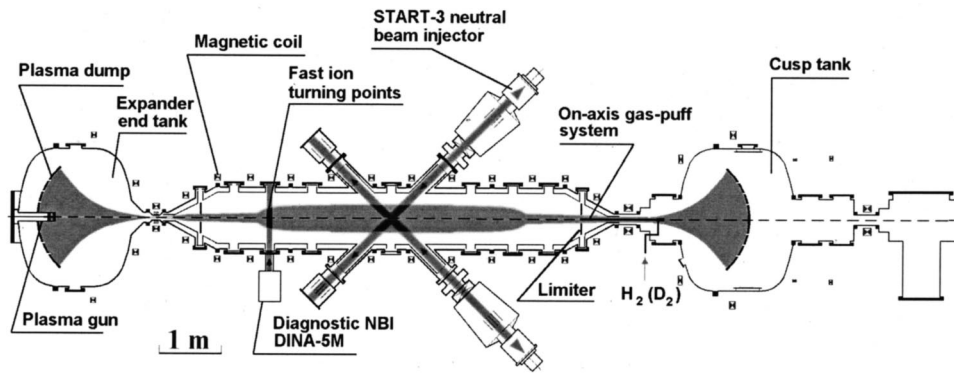


FIG. 1. The GDT layout.

measurements. The neutral beam injector is mounted on an alignment flange (see Fig. 2) to provide capability to change the beam direction. In the experiments described here the beam direction was fixed perpendicular to the axial magnetic field in GDT, but in the future the beam will be moved to make axial profile MSE measurements.

Two diagnostic ports are used for observation, as shown in Fig. 2. The upper port corresponds to the angle $\Theta=22.5^\circ$ between the beam and the viewing chord, the lower one corresponds to $\Theta=45^\circ$. The latter observation geometry was chosen for the present experiments because the achievable spatial resolution is better (4.5 cm radial \times 1.5 cm axial), an essential requirement for magnetic-field profile measurements. For the 22.5° observation angle, the spatial resolution is 8×1.5 cm. Despite poorer spatial resolution, the smaller observation angle has several advantages: (1) a higher signal-to-noise ratio due to the larger intersection volume of the beam and viewing solid angle, and (2) better separation between the π and σ components of the measured spectrum due to a higher degree of σ -polarized emission rejection. Since both these factors provide for better measurement accuracy, initial MSE measurements were made at $\Theta=22.5^\circ$. (Figure 4 shows an example spectrum with the π^+ and π^- manifolds clearly resolved.)

The optical system⁸ consists of a light collection telescope with a ferroelectric liquid crystal (FLC) shutter, and a spectrometer with a charge-coupled device (CCD) detector controlled by a personal computer. The FLC shutter linearly

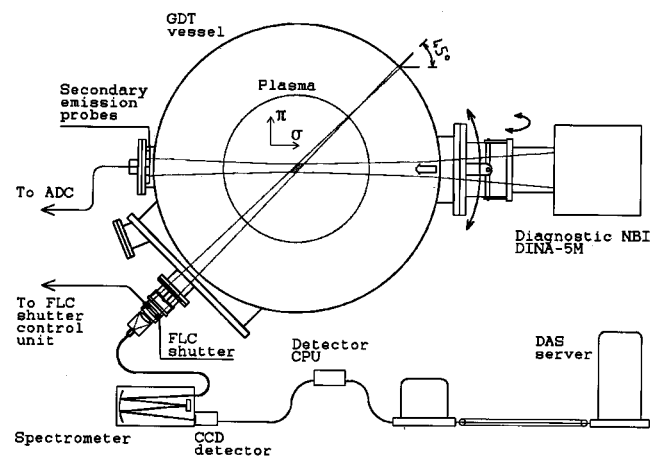


FIG. 2. Layout of the MSE diagnostic on GDT (polarization directions of π and σ components of emitted radiation are shown).

polarizes the collected light, thus eliminating the need for a separate polarizing component. It was opened so as to collect light only during the 200 μ s beam pulse. The collected beam emission was polarized perpendicular to the viewing chord and in the plane of Fig. 2, accordingly the intensities of the π and σ components at $\Theta=45^\circ$ are similar. The measured spectrum was digitized by the CCD controller and stored in an archive of the common GDT data acquisition system. For calibration of the spectrometer dispersion we used two clearly observable lines emitted from core plasma: H α at 656.28 nm and C II at 657.81 nm (see Fig. 5). The Doppler-shifted beam emission line, which undergoes the Stark splitting, was visible in the same wavelength range for both observation angles without readjustment of the spectrometer. To improve the signal-to-noise ratio we summed up several measured spectra (up to 10) in a series of shots with reproducible parameters.

The spectrum in Fig. 5 was recorded on the target plasma without neutral beam heating. It can be also used for checking of diagnostic technique accuracy, since the diamagnetic perturbation of magnetic field is negligibly low in this regime (less than 1%). The calculated $|B|$ of 0.493 T is close to the vacuum field value 0.494 T.

III. RADIALLY RESOLVED MEASUREMENT OF $|B|$ ON THE GAS-DYNAMIC TRAP

The GDT cross section where the diagnostic was located corresponds to the volume of the fast ion turning point (mirror ratio $R=2$). The plasma pressure and diamagnetic magnetic-field perturbation are maximized at this location.

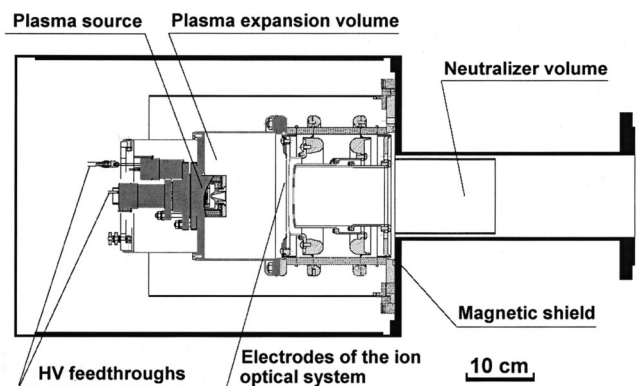


FIG. 3. Schematic of the DINA-5M diagnostic neutral beam injector.

TABLE I. The parameters of DINA-5M injector.

Type of ion optical system	Focusing
Energy of injection	40 keV
Extracted ion current (hydrogen)	Up to 7 A
Pulse duration	200 μ s
Focal length	1.3 m
Beam radius at focal plane	2 cm
Current density at focal plane	0.25 A/cm ²
Beam current fraction with full injection energy	93.6%

The hydrogen target plasma in the present experiments was produced by a plasma gun pulse of ≈ 2.8 ms duration (see Fig. 1). The fast ion population was created by deuterium neutral beam injection of power up to 3.9 MW for 1 ms duration. Plasma magnetohydrodynamic stability was provided by expanders (see Fig. 1) and biased limiters. Typical target plasma parameters at the end of the heating beam pulse were 100 eV electron temperature at a density of $3 \times 10^{19} \text{ m}^{-3}$. Estimates from previous experiments suggest that the fast ion population has a pressure ratio $p_{\text{fast}}/p_{\text{target}} \approx 10$ and perpendicular $\beta \approx 30\%$ in the turning point area.⁹ In order to measure the maximum diamagnetic perturbation of $|\mathbf{B}|$, the 200 μ s diagnostic neutral beam pulse was fired at the end of heating beam pulse.

The measured radial profile of $|\mathbf{B}|$ is shown in Fig. 6. Horizontal error bars are defined by the spatial resolution of 4.5 cm. The error in the measured value of $|\mathbf{B}|$ is due to

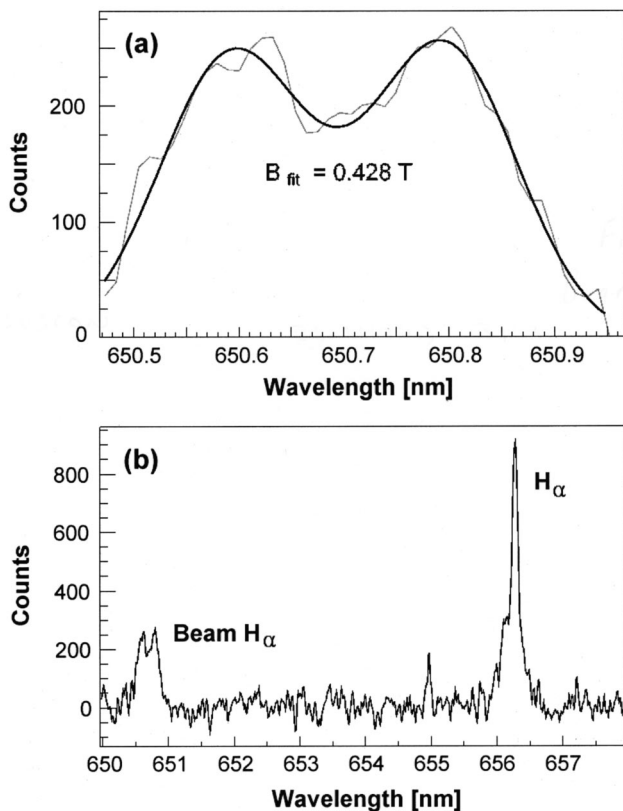


FIG. 4. A typical motional Stark spectrum from GDT recorded at $\Theta = 22.5^\circ$. (a) A spectrum of beam H_α emission and a fit curve (bold line). (b) A full-scale spectrum summed up over six shots.

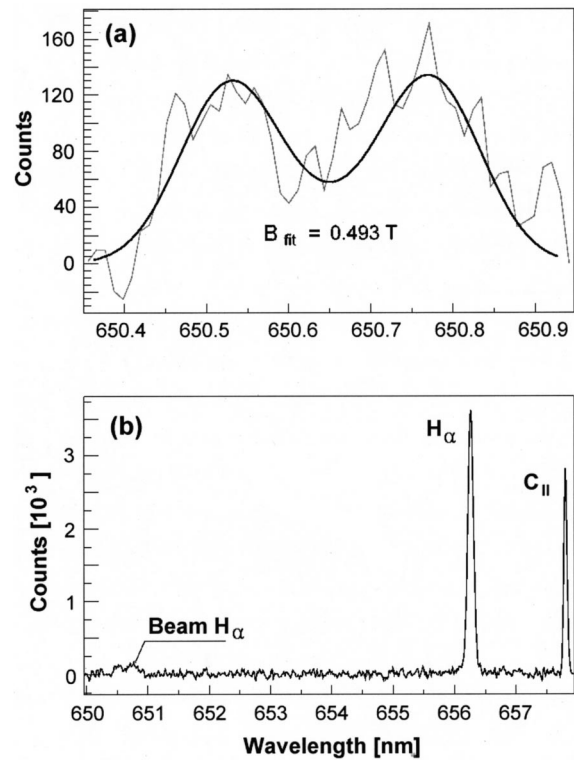


FIG. 5. A motional Stark spectrum recorded on the target plasma at $\Theta = 22.5^\circ$. (a) A spectrum of beam H_α emission and a fit curve (bold line). The measurement result of 0.493 T is close to the vacuum field value of 0.494 T and within the measurement accuracy. (b) Spectrum averaged over four shots. Plasma emission lines H_α and C_{II} were used for calibration of the spectrometer dispersion.

several factors: shot-to-shot fluctuation of plasma parameters, variation of the beam injection energy, uncertainty in the dispersion calibration, and statistical (Poisson) fluctuation of the recorded beam emission. The fluctuation of plasma parameters (in a series of shots corresponding to the same regime) contributed an uncertainty $\approx 2\%$, and the uncertainty due to statistical fluctuation $\approx 3\%$. The other two factors contributed negligibly to the uncertainty of measured

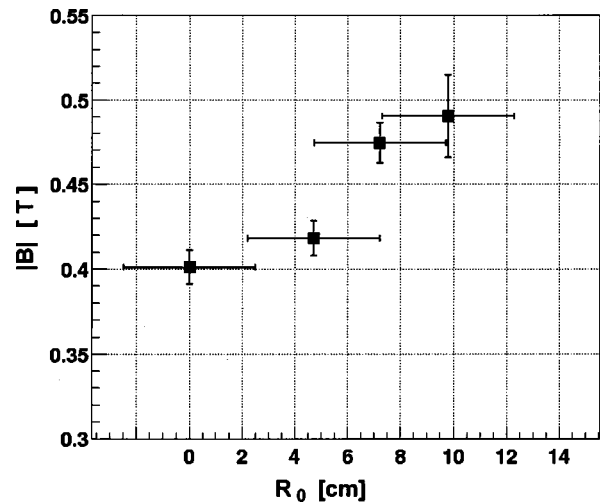


FIG. 6. Radial profile of $|\mathbf{B}|$ mapped onto the GDT midplane. Horizontal error bars show the spatial resolution of the diagnostic.

$|\mathbf{B}|$. The precision of the MSE measurements of $|\mathbf{B}|$ is estimated as 4%, and was cross checked by calculation of the statistical deviation in results obtained in separate sets of shots. Further analysis of this radial profile of $|\mathbf{B}|$ is currently under way and is expected to result in an increased understanding of fast ion physics in a gas-dynamic trap axial mirror system.

IV. SUMMARY

Spectral motional Stark measurements of $|\mathbf{B}|$ have been accomplished on the Gas-Dynamic Trap magnetic mirror device. Operational characteristics of the diagnostic beam and optical system provide the capability to make measurements in low fields ($|\mathbf{B}| \approx 0.4 \div 0.5$ T) with spatial resolution of 4.5 cm radial \times 1.5 cm axial for an observation angle $\Theta = 45^\circ$,

and temporal resolution of 200 μs . The precision of spatially resolved measurements of $|\mathbf{B}|$ is estimated as 4%.

¹P. A. Bagryansky *et al.*, Trans. Fusion Technol. **35**, 79 (1999).

²D. D. Ryutov, Plasma Phys. Controlled Fusion **32**, 999 (1990).

³P. A. Bagryansky, D. J. Den Hartog, G. Fiksel, A. A. Ivanov, S. A. Korepanov, A. A. Lizunov, and V. Ya. Savkin, Europhysics Conference Abstracts 25A, 1217 (2001), on CD-ROM.

⁴W. Mandl, R. C. Wolf, M. G. von Hellermann, and H. P. Summers, Plasma Phys. Controlled Fusion **35**, 1373 (1993).

⁵D. Craig, D. J. Den Hartog, G. Fiksel, V. I. Davydenko, and A. A. Ivanov, Rev. Sci. Instrum. **72**, 1008 (2001).

⁶R. Jaspers, B. S. Q. Elzendoorn, A. J. Donné, and T. Soetens, Rev. Sci. Instrum. **72**, 1018 (2001).

⁷S. A. Korepanov, P. A. Bagryansky, P. P. Deichuli, A. A. Ivanov, and Yu. A. Tsidulko, Trans. Fusion Technol. **35**, 345 (1999).

⁸D. J. Den Hartog and D. J. Holly, Rev. Sci. Instrum. **68**, 1038 (1997).

⁹A. V. Anikeev *et al.*, Nucl. Fusion **40**, 753 (2000).